C-Heterogenized Re Nanoparticles as Effective Catalysts for the Reduction of 4-Nitrophenol and Oxidation of 1-Phenylethanol

Ana P. C. Ribeiro [1,*], Beatriz M. Santos [1], Rute F. C. Faustino [1], Armando J. L. Pombeiro [1,2] and Luísa M. D. R. S. Martins [1,*]

[1] Centro de Química Estrutural, Institute of Molecular Sciences, Departamento de Engenharia Química, Instituto Superior Técnico, Universidade de Lisboa, 1049-001 Lisboa, Portugal

[2] Research Institute of Chemistry, Peoples' Friendship University of Russia, (RUDN University), 6 Miklukho-Maklaya Street, 117198 Moscow, Russia

* Correspondence: apribeiro@tecnico.ulisboa.pt (A.P.C.R.); luisammartins@tecnico.ulisboa.pt (L.M.D.R.S.M.)

Abstract: Rhenium nanoparticles (Re NPs) supported on Norit (activated carbon—C) and graphene (G) were prepared by a solvothermal method under microwave irradiation (MW). The synthesised heterogeneous catalysts were characterised and tested as reduction and oxidation catalysts, highlighting their dual catalytic behaviour. In the first case, they were used, for the first time, to reduce 4-nitrophenol, in aqueous medium, under MW irradiation. Re catalysts were easily recovered by centrifugation and recycled up to six times without significant activity loss. However, the same Re catalysts in MW-assisted oxidation of 1-phenylethanol with no added solvent experienced a significant loss of activity when recycled. The higher activity of the rhenium nanoparticles supported on graphene (Re/G) catalyst in both reactions was assigned to the higher dispersion and smaller particle size of Re NPs when graphene is the support.

1. Introduction

Most of the reported preparation methods for immobilised metal catalysts require treatment of the supports and the use of solvents. In addition, there is the usual difficulty of controlling the preparation steps and obtaining highly dispersed catalysts. The microwave-assisted (MW) method [1], which is often more environmentally friendly than wet preparation methods as it exhibits better heat transfer effect than conventional methods [2], has been reported by several authors for the synthesis of supported catalysts [3].

Many industrial catalysts are formed with expensive transition metals dispersed in inexpensive, high-area porous substrates. Supported metal catalysts can be dispersed into nano-sized clusters to improve the efficiency of catalytically active atoms. If the cluster size is small enough, most atoms that are on the surface are accessible to reactants and available for catalysis [4]. Since low-coordination or unsaturated atoms often work as active sites, small size clusters of atoms, whenever possible, are highly desirable for catalytic reactions [5].

Rhenium is a very promising element to be used as a versatile catalyst. Apart from bare metal, rhenium nanoparticles (Re NPs) can serve as catalysts when supported on polymers [6], in DNA scaffold [7], carbon [8], γ-Al$_2$O$_3$ [9], etc. For example, Ni et al. successfully prepared supported rhenium catalysts by the microwave-assisted thermolytic method, and the as-prepared catalysts showed good catalytic properties in the hydrogenation of cinnamaldehyde [10]. The hydrogenation of succinic acid over

supported rhenium catalysts, prepared by the same method, was already performed efficiently [11].

4-Nitrophenol (4-NP) is an important secondary product obtained from the pharmaceutical industry, synthetic dyes, pesticides and herbicides. It is recognized as a hazardous product and its removal from the environment is a mandatory objective due to its toxicity to human and animal blood, as well as to various organs [12–14]. Therefore, its catalytic reduction with different NPs has been the subject of on-going research [15–17]. The conversion of a nitro group to amino is mainly achieved by treatment with various reducing reagents, such as $NaBH_4$ [18], H_2 and CO gas [19], N_2H_4 [20], ammonia-borane (NH_3BH_3) [21] or triethylsilicon hydride (Et_3SiH) [22], under acidic/ neutral/basic conditions.

Among the above-mentioned reducing agents, $NaBH_4$ is often used as a mild and selective one, providing a favourably economic option for reduction reactions under normal pressure and room temperature in the presence of transition metal catalysts [23].

The reduction of 4-NP to 4-aminophenol (4-AP) is a six-electron process with a 44 kJ mol^{-1} activation energy. Due to the high activation energy, this reduction with $NaBH_4$ requires the use of a catalyst to aid in the production of an active hydrogen source [24].

On the other hand, this reaction can occur at room temperature/pressure and using water as solvent. Since 4-NP has a light-yellow colour and 4-AP is colourless, this reaction can be quantitatively monitored by ultraviolet–visible light (UV-vis) spectrophotometry. The large excess of $NaBH_4$ used makes the reaction follow pseudo first-order kinetics [25,26]. Studies have been extensively reported for nanoparticles, such as supported palladium NPs, but rarely on supported Re NPs.

Rhenium complexes have become relevant catalysts in the oxidation of various organic compounds, such as olefins [27], ketones [28,29] and alcohols [30]. High valent oxo-rhenium complexes have also been successfully used in the activation of C-H bonds of aromatic and saturated hydrocarbons [31–38]. Molecular oxygen or peroxides are often preferred as oxidising agents. The first, employed by enzymes in biological processes, represents the greenest choice; however, its application in laboratory reactions is not easily controllable, not infrequently resulting in overoxidized products. In addition, the low toxicity and low/moderate cost of peroxides such as hydrogen peroxide or tert-butyl hydroperoxide (TBHP), and the nature of their by-products (water and alcohol, respectively), make them sustainable reagents [28,39].

Regarding the reaction medium, recently the progressive growth of awareness of environmental issues has stimulated remarkable efforts toward the use of green solvents [40] including water, or the achievement of solvent-less conditions.

In this work, supported rhenium nanoparticles (Re NPs) were prepared by a microwave (MW)-assisted method, and their catalytic activity was investigated under MW irradiation, in aqueous media, for the reduction of 4-nitrophenol (4-NP) to 4-aminophenol (4-AP), and under solvent–free conditions for the oxidation of 1-phenylethanol to acetophenone. The textural and structural properties of the supported Re catalysts were characterised and discussed along with their catalytic performance and the kinetics of the catalysed reduction reaction.

2. Results and Discussion

2.1. Characterization of Re/C and Re/G Catalysts

In this work, supported rhenium catalysts were prepared with the MW-assisted thermolytic method by using decacarbonyldirhenium [$Re_2(CO)_{10}$] as a precursor. The chosen supports were Norit (C) and graphene (G), tried herein for the first time with a Re precursor, leading to Re/C and Re/G, respectively. The chosen MW methodology was effective in the incorporation of Re amounts very close to the theoretical (1 wt.%) loadings (0.97 wt.%. for Re/C and 0.99 wt.% for Re/G), as determined by inductively coupled plasma atomic emission spectroscopy (ICP-AES) (see Section 3).

The textural and structural properties of the catalysts were characterised and associated with their catalytic performance in the reduction of 4-nitrophenol and the oxidation of 1-phenylethanol.

The structural characterization based on powder X-ray diffraction patterns reveals that Norit and graphene present two peaks at $2\theta = 24.6°$ and $44.6°$, which can be attributed to the amorphous graphitic carbon (002) and (100), respectively (Figure 1a) [40].

According to standard X-ray diffraction patterns (JCPDS no. 05-0702), diffraction peaks at $2\theta = 42.9, 40.5$ and $37.6°$ should be observed in these catalysts, which were indexed as the (101), (002) and (100) planes of metallic Re. However, Figure 1b reveals that no discernible characteristic diffraction peak due to metallic Re was observed apart from the diffraction peaks of active carbon. This indicates that the rhenium particles are too small to be resolved (less than 4 nm, see below microscopic characterization) and/or highly dispersed on the surface of the carbon material. In addition, the characteristic diffraction peaks of Re are close to that with higher 2θ of active carbon, which would lead to the covering of the Re peaks. Similar difficulties were reported by Xin Di et al. [11] for their carbon supported Re NPs formed under MW irradiation.
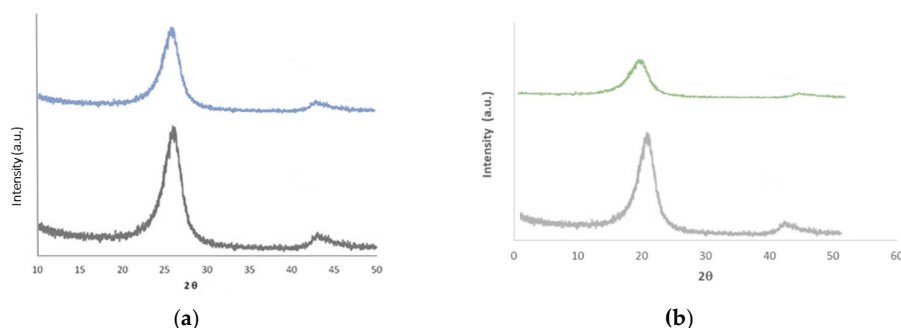
Figure 1. Powder X-ray diffraction (XRD patterns of (**a**) the initial supports Norit (lower) and graphene (upper), and (**b**) supported Re NPs in Norit (Re/C—lower) and graphene (Re/G—upper).

To further investigate the structure and composition distribution of our C-supported Re materials, scanning electron microscopy (SEM), transmission electron microscopy (TEM) images and energy dispersive spectroscopy (EDS) spectrums of Re/C, Re/G and respective supports were obtained. SEM images of Norit and graphene (Figure 2a and 2b, respectively) show a remarkable difference in the morphology of the two carbon types. The TEM image (Figure 2c) confirmed the presence of the Re nanoparticles exhibiting their non-symmetrical shapes with a particle size ranging from 1 to 4 nm. Thus, the catalysts prepared by MW irradiation showed better dispersion and smaller particle size than other C-supported Re catalysts. This behaviour was previously found by Xin Di et al. [11]. However, one should be careful with the duration of the MW irradiation, as for longer irradiation times, the agglomeration of particles takes place, likely as a result of the extra energy provided by the MW irradiation.

(a)

(b)

(c)
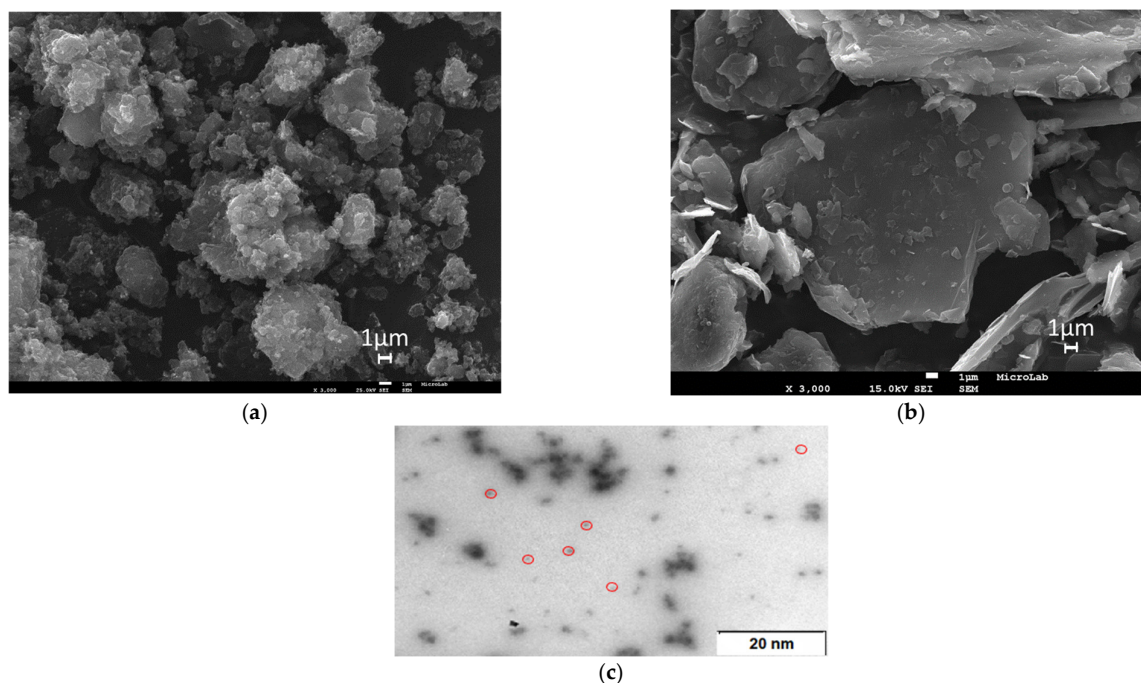
Figure 2. SEM, TEM images and EDS. (**a**) SEM image of Norit; (**b**) SEM image of graphene; (**c**) TEM image of Re NPs on a sheet of graphene (red circles highlight the Re NPs).

2.2. Reduction of 4-Nitrophenol Using Re/C and Re/G Catalysts

The reduction of 4-NP to 4-AP, catalysed by Re/C and Re/G catalysts (Scheme 1), was monitored by UV-Vis spectroscopy (Figure 3).
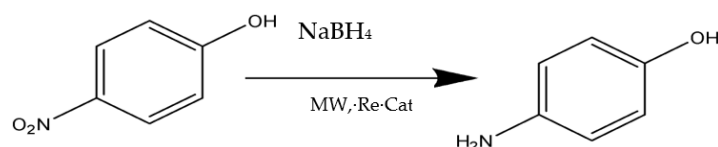
Scheme 1. Reduction of 4-NP to 4-AP.

The 4-NP solution exhibits a clear absorption maximum at λ = 380 nm; however, the peak shifted to λ = 400 nm immediately after the addition of $NaBH_4$ solution [41]. The resulting colour change to bright yellow was due to the formation of a 4-nitrophenolate ion (4-NP$^-$) [41]. The maximum absorption peak at λ = 400 nm did not change over time, even with an excess of $NaBH_4$, and small bubbles of H_2 gas were generated from the reduction of $NaBH_4$ with water according to Equation (1) [41]:

$$NaBH_4 + 2\,H_2O \rightarrow NaBO_2 + 4\,H_2 \tag{1}$$
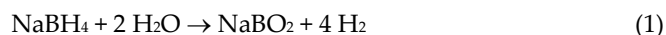
The reduction of 4-NP (E^0 = −0.76 V) by $NaBH_4$ (E^0 = −1.33 V) is thermodynamically feasible, but kinetically restricted in the absence of a catalyst [41,42] in aqueous $NaBH_4$. Our results confirm that the reaction does not proceed in a pure aqueous $NaBH_4$ solution.

The addition of catalyst to the reaction mixture led to the decrease in the peak intensity of the 4-nitrophenolate ion with the appearance and growth of the absorption peak of 4-aminophenol at 300 nm. The observation of isosbestic points demonstrates that no side products were produced. Figure 3b shows the absorption dependence at the wavelength of 400 nm over time for the reduction of 4-nitrophenolate ions. In the present catalytic system, contrary to what was observed by other authors [41], no induction time was noticed. Such a reported induction period was linked [41] to the level of dissolved oxygen in

the reaction medium, [42–46] and it ended once the level fell below a critical value that was dependent upon the metal nanoparticles used as the catalyst.

The linear fitting of $\ln(A/A_0)$ versus time follows pseudo first-order kinetics. The apparent kinetic rate constant (k_{app}) was determined from linear regression using the Equation (2):

$$ln(\frac{A}{A_0}) = \ ln(\frac{C}{C_0}) = - \ k_{app} \ \cdot t \tag{2}$$

where A_0 is the initial absorbance, and A is the absorbance of the 4-nitrophenolate ion at every time point. C_0 is the initial concentration, and C is the concentration of 4-nitrophenolate ion [4NP] in the reaction medium, and t is the reaction time. According to the slope, the apparent rate constant values are presented in Table 1.

Table 1. Catalytic performance [a] of Re/C and Re/G as a function of catalyst amount and temperature.

Entry	Catalyst	Cat. Amount [b]	T	$k_{app} \times 10^3$	$[4NP] \times 10^3$
		(μmol of Re)	(°C)	(s^{-1})	(M)
1		0.2	35	1.34	3.36
2	Re/C	0.02		1.47	3.10
3		0.2	50	1.37	3.30
4		0.02		1.58	2.91
5		0.2	35	1.36	3.32
6	Re/G	0.02		1.53	2.99
7		0.2	50	1.45	3.14
8		0.02		1.62	2.84

[a] Conditions: 15 W power, reaction time up to 30 min. [4-NP] = 7.5 × 10^{-3} M; [NaBH$_4$] = 0.169 M. [b] Molar amount of Re supported at the carbon material (graphene or Norit).

The bare Norit and graphene showed no catalytic activity for the reduction of 4-NP to 4-AP and only trace amounts of 4-AP were detected over a reaction time of 30 min (Table S2, entries 1 and 2, ESI). In addition, the same reaction was attempted using the rhenium NPs precursor [Re$_2$(CO)$_{10}$] as the catalyst, but no conversion of 4-NP was observed. A possible explanation for the catalytic inactivity of the Re compound is its insolubility in water [41], which impaired its action in the reduction reaction in the used aqueous efficiency. Attempts to further increase the amount of catalyst used in the reaction were not successful since the amount of carbon present prevented the observation of clear UV spectra.


(a)

(b)

(c)　　　　　　　　　　　　　　　(d)
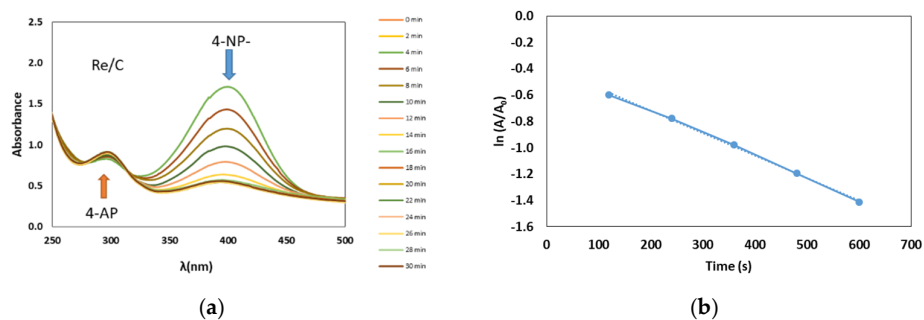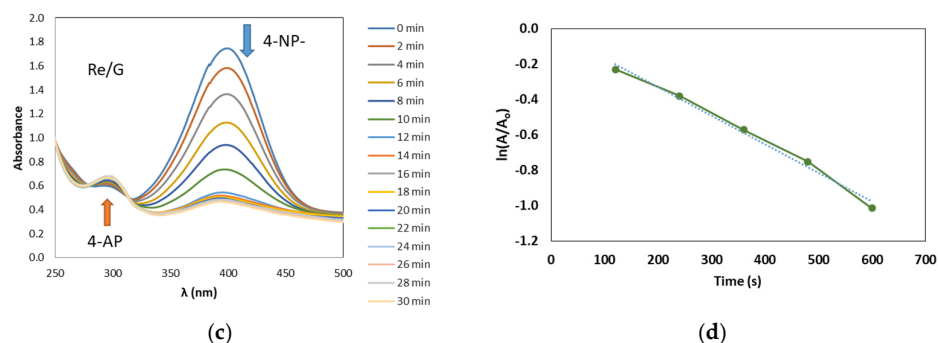
Figure 3. Reduction of 4-NP to 4-AP (**a**,**c**) Monitoring UV-Vis absorption spectra (2 min intervals) for the catalytic reduction of 4-NP using supported Re nanoparticles (Re/C and Re/G, respectively). (**b**,**d**) Absorption dependence on time. Conditions: 15 W power, [4-NP] = 7.5×10^{-3} M; [NaBH$_4$] = 0.169 M; n Re/C = n Re/G = 0.2 μmol of Re immobilized at the carbon support; T = 50 °C.

The different electron transfer kinetics that occurs in the carbon materials could be possibly ascribed to the synergetic effects of the surface chemistry (e.g., C/O ratio, presence of functionalized groups, surface charge, or surface cleanness) and conductivity of the materials. A main difference between Norit and graphene is that graphene (with a single thin layer 2D film of carbon**)** has a greater surface area than Norit [47]**,** leading to a better dispersion of the nanoparticles. This explains the difference in their activity.

Recycling of the catalysts Re/C and Re/G was performed by recovering them by centrifugation, filtration, washing and drying prior to a new use. After the 6th cycle (Figure 4 for Re/G catalyst), the conversion decreased, most likely due to leaching of rhenium from the carbon support.
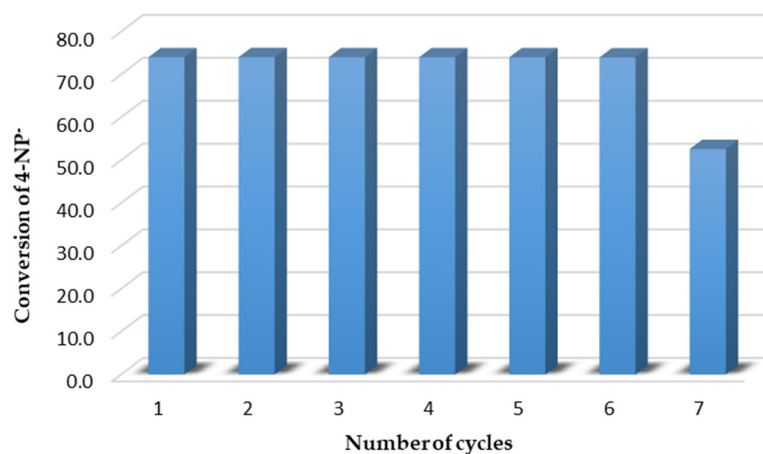
Figure 4. Recycling studies for the reduction of 4-NP to 4-AP, using Re/G as catalyst (0.2 μmol of Re immobilized at the carbon support; T = 50 °C; 15 W power; [4-NP] = 7.5×10^{-3} M; [NaBH$_4$] = 0.169 M.

A comparison with previous studies shows that our highest value of k_{app}, which is for Re/G (entry 8, Table 1), is much lower than those for Re/OMC (ordered mesoporous carbon), ca. 0.15 s^{-1} [7], for similar amounts, and slightly lower than those for other carbon matrix-supported Ag NPs, ca. 5.3×10^{-3} s^{-1} [8]. However, for all our catalysts, it surpasses those of Re nanoclusters (0.06 min^{-1}) [8].

2.3. Mechanistic Considerations

The kinetic investigation of this reaction suggests that both reactants (BH$_4^-$ and 4-NP) adsorb on the surface of Re NPs, and the reaction can be modelled through the Langmuir–Hinshelwood mechanism [26]. For the first step of this proposed mechanism, 4-NP molecules are converted to 4-nitrophenolate ions (4-NP$^-$) in the presence of NaBH$_4$ with the formation of H$_2$ (Equation (1) and Scheme 2). The interaction of borohydride with the catalyst would also provide the necessary hydrogen for the reduction of 4-NP [24]. Active hydrogen atoms can also be formed on the surface of the nanocomposite, due to reduction of water [25]. 4-Nitrophenolate ions are adsorbed on the surface of the catalyst and reduced to 4-nitrosophenol as an intermediate, which is further reduced to 4-(hydroxylamino)phenol as stable intermediate. Further reduction and product removal from the surface of the nanocomposite provides the free NP surface for the catalytic cycle.

Assuming that the borohydride group desorbs irreversibly and does not impact the reaction rate, and that the reactants sorption and desorption steps are not rate determining, the kinetic expression can be simplified to a pseudo-first order reaction rate [25].
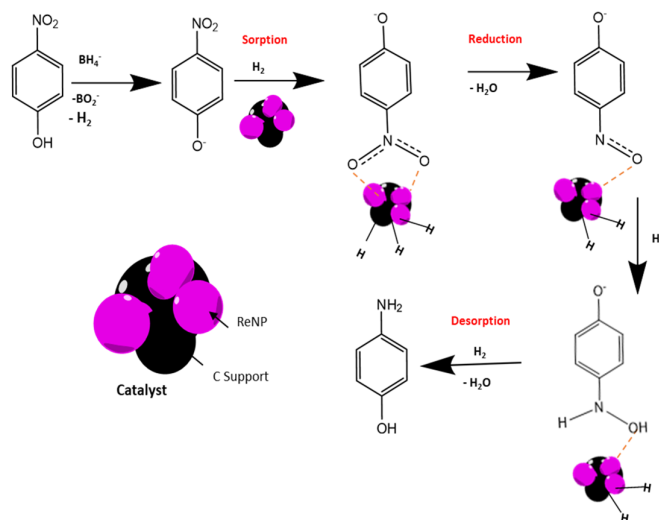
Scheme 2. Proposed 4-NP reduction mechanism using NaBH$_4$ as the reducing agent—Reproduced from [25], John Wiley & Sons Ltd: 2017.

2.4. Phenylethanol Oxidation Using Re/C and Re/G Catalysts

To evaluate the performance of the above rhenium species in homogeneous and heterogenous oxidative catalysis, we tested and compared the catalytic properties of the parent rhenium complex [Re$_2$(CO)$_{10}$] with those of the newly synthesized Re/C and Re/G NPs for the MW-assisted oxidation of 1-phenylethanol to acetophenone (Scheme 3, Tables 2 and 3).
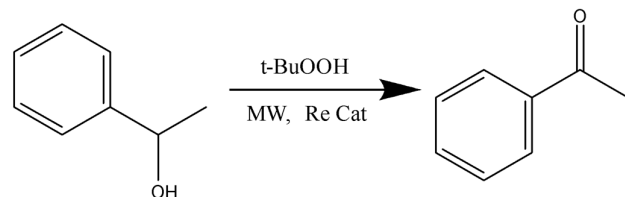
Scheme 3. 1-Phenylethanol oxidation, under MW radiation, catalysed by supported Re NPs (Re/C and Re/G).

The reactions were performed using TBHP as the oxidizing agent and MW heating which had been successfully employed in previous studies [42–46]. The heterogeneous

catalysis was performed under the best conditions (50 °C and 60 min, entry 9 of Table 2) obtained in the homogeneous studies, for comparative purposes. In addition, reactions conducted with the supports (only) as possible catalysts did not lead to any significant amount of product (see Table S2, ESI).

Table 2. MW-assisted oxidation of 1-phenylethanol catalysed by [Re$_2$(CO)$_{10}$] (homogeneous conditions) [a].

Entry	Cat. Amount	Temp.	Time	Yield [b]	TON [c]	TOF [d]
	(µmol of Re)	(°C)	(min)	(%)		(h^{-1})
1	0	50	60	0.9	-	-
2	2	50	60	44.8	1.12×10^3	1.12×10^3
3	10	50	5	9.8	49	588
4	10	50	10	11.3	57	339
5	10	50	15	12. 9	65	258
6	10	50	30	72.5	363	725
7	20	35	30	10.7	27	54
8	20	50	30	65.0	163	325
9	20	50	60	98.8	247	247
10	20	80	30	15.2	38	76
11	20	80	60	57.2	143	143

[a] General reaction conditions: 15 W power, TBHP (10 mmol), 1-phenylethanol (5 mmol). [b] Yield (%) = moles of product(s) per 100 moles of substrate. [c] Turnover number (TON) = moles of product(s) per mole of Re. [d] Turnover frequency (TOF) = TON/reaction time.

Table 3. MW-assisted oxidation of 1-phenylethanol in heterogeneous conditions (catalysed by Re/C or Re/G) [a].

Entry	Catalyst	Cat. Amount	Yield [b]	TON [c]
		(µmol of Re)	(%)	or TOF (h^{-1}) [d]
1		0.02	54.3	1.36×10^5
2	Re/G	2	30.6	765
3		20	20.8	52
4		0.02	43.7	1.09×10^5
5	Re/C	2	22.4	560
6		20	18.1	45

[a] General reaction conditions: 15 W power, 50 °C, 60 min of irradiation, TBHP (10 mmol), 1-phenylethanol (5 mmol). [b] Yield (%) = moles of product(s) per 100 moles of substrate. [c] Turnover number (TON) = moles of product(s) per mole of supported Re catalyst. [d] Turnover frequency (TOF) = TON/reaction time.

For the same metal catalyst loading, the homogeneous conditions led to better results than the heterogeneous ones, in terms of yields. TONs, on the other hand, when applied to 0.02 µmol of Re, were proven to be significantly higher on the heterogeneous case. This is possibly due to the higher activity of the loaded rhenium present at the surface of the catalyst. Therefore, the surface can have an important role, since the 2D surface of graphene can have a stabilising effect on the nanoparticles, making them more accessible and reactive. Increasing the amount of catalyst, in the heterogeneous case, leads to a decrease in yield, in contrast to what occurs in the homogeneous catalytic system. Increasing the amount of metal catalyst in the heterogeneous case requires the use of a larger amount of support which can affect the catalytic activity of the system**.**

Recycling experiments for Re/G were carried out, but the best results, reported in Table 4, are not as good as in the homogeneous system. This could be due to the following reasons: (i) the formation of rhenium oxide at the surface of the supported catalysts, that would decrease their activity; or (ii) the occurrence of lixiviation of Re NPs from the support surface, leaving less or no metal available for the catalytic cycle.

Table 4. Recycling studies [a] of Re/C or Re/G as heterogeneous catalysts for the MW-assisted oxidation of 1-phenylethanol to acetophenone.

Entry	Catalyst	Yield [b](%)	TON [c] or TOF (h^{-1}) [d]
1		30.6	765
2	Re/G	6.3	158
3		0.5	13
4		22.4	560
5	Re/C	2.6	65
6		0.6	15

[a] General reaction conditions: 15 W power, 50 °C, 60 min of irradiation, catalyst (2 μmol of Re immobilized at the carbon support), TBHP (10 mmol), 1-phenylethanol (5 mmol); [b] Yield (%) = moles of product per 100 moles of substrate. [c] Turnover number (TON) = moles of product per mole of supported Re catalyst. [d] Turnover frequency (TOF) = TON/reaction time.

The ICP-AES analysis of the recovered catalysts after the second consecutive run has shown that no rhenium remained in the sample, which indicates that the type of interaction between Re NPs and both carbon supports is weak.

In addition, only traces of acetophenone were found in a run performed with the filtered solution from the first cycle performed in conditions of entry 1 of Table 3, taken to dryness, to which new standard portions of all other reagents were added. This suggests the formation of Re inactive species upon the release from graphene.

Oxidation of 1-phenylethanol by rhenium complexes is a virtually unexplored area, to the best of our knowledge. Although oxidation of alcohols catalysed by rhenium has been reported previously, no direct comparison can be made with our values, in view of the different types of catalysts and conditions that were used. In fact, some oxo-rhenium (V and VII) complexes using bis(4-chlorophenyl) sulfoxide as oxidant, in refluxing toluene, catalysed the oxidation of primary and secondary alcohols in high yields (up to 94%) using 10% molar load of Re, for a reaction time interval of 17–24 h, attaining a maximum TON value of 10 for 17 h of reaction time [41], which indicates a less active catalyst that ours. Among the secondary alcohols, derivatives of 1-phenylethanol (bearing strong electron-withdrawing substituents) were used as substrates, but not the unsubstituted 1-phenylethanol itself [46].

Bipyridine iron complexes were reported [48] to catalyse the oxidation of 1-phenylethanol with hydrogen peroxide in water, using either microwave or conventional heating. For the reaction time of 30 min and at 100 °C, the maximum yield (82%) was obtained by adding an acidic buffer to the acetonitrile solvent, and values of TON of 82 and TOF of 164 h^{-1} were achieved, which are lower than ours (although for 1 h but at a lower temperature). The oxidation under microwave irradiation of 1-phenylethanol using an iron(II) tris(pyrazolyl)methane catalyst supported at different carbon materials (functionalized multiwalled carbon nanotubes or nanodiamonds) has been studied [49–51], and the catalyst was shown to undergo recycling without losing its high catalytic activity. The carbon supports and the catalyst were quite different from those of the current work. For 5 μmol of supported catalyst on multiwalled carbon nanotubes, a maximum TON of 1182 was achieved for 0.5 h of reaction time [49], thus indicating a high catalytic activity. For the same Fe catalyst supported on nanodiamonds, a 97% yield of acetophenone and a TOF of 9.7×10^2 h^{-1} were obtained after 1 h of MW irradiation (25 W) at 80 °C [51], i.e., at higher power and temperature than those in the current work.

3. Materials and Methods

All reagents were purchased from Sigma-Aldrich (Munich, Germany) and used as received. Solvents were purified, when necessary, by standard methods and freshly distilled under dinitrogen immediately prior to use. The graphene was prepared and characterized according to a published method [12].

The synthesized graphene and the rhenium NPs supported on the carbon materials (Norit and graphene) were characterized by X-ray diffraction (XRD), scanning electron microscopy (SEM), energy dispersive spectroscopy (EDS) and transmission electron microscopy (TEM). Morphology and distribution of the support and the catalysts were characterized using a SEM (JEOL 7001F with Oxford light elements EDS detector and EBSD detector, JEOL, Tokyo, Japan). X-ray diffraction spectra were obtained at a Bruker D8 ADVANCE Powder Diffractometer (Bruker Corporation, Billerica, MA, USA), with Cu radiation in a Bragg Brentano geometry. The rhenium content of supported catalysts was analysed by inductively coupled plasma atomic emission spectroscopy (ICP-AES) carried out by Laboratório de Análises of IST using an ICP-AES model Ultima (Horiba Jobin-Yvon, Kyoto, Japan) apparatus, before and after the catalytic reactions.

Catalytic reactions under microwave (MW) irradiation were performed in a focused Anton Paar Monowave 300 reactor (Anton Paar GmbH, Graz, Austria) fitted with an IR temperature detector, and a rotational system, in a Pyrex cylindrical tube (10 mL capacity, 13 mm internal diameter). UV measurements were performed in a Lambda 35, Perkin Elmer (Waltham, MA, USA). Gas chromatographic (GC) experiments were run at a FISONS Instruments GC 8000 series gas chromatograph equipped with a flame ionization (FID) detector and a capillary column (DB-WAX, column length of 30 m; column internal diameter of 0.32 mm) and run by the software Jasco-Borwin v.1.50 (Jasco, Tokyo, Japan). He was the carrier gas. The temperature of injection was 240 °C. After injection, the reaction temperature was maintained at 140 °C for 1 min, then raised, by 10 °C/min, to 220 °C and held for 1 min at this temperature. All products were identified by comparing their retention times with known reference compounds.

3.1. Catalyst Preparation

Supported rhenium catalysts were prepared according to the microwave-assisted thermolytic method described by Di et al. [11], by using decacarbonyldirhenium $[Re_2(CO)_{10}]$ as a precursor. In a brief description, the $[Re_2(CO)_{10}]$ and the carbon material (Norit or graphene) were simultaneously added into an agate mortar and then mechanically mixed for 30 min. The homogeneous mixture was transferred into a borosilicate tube reactor, which was then placed in a microwave reactor. The homogeneous mixture was set at 800 W power for 1 min and then kept at 100 W for 4 min. Finally, the reaction mixture was cooled to room temperature.

3.2. Catalytic Reduction of 4-Nitrophenol

The catalytic reduction of 4-nitrophenol (4-NP) to 4-aminophenol (4-AP) in the presence of Re/G or Re/C and sodium borohydride as a reductant was previously described [52–54]. Briefly, the UV absorption measurements were performed in a 3 mL quartz cell. The solutions of 4-NP and $NaBH_4$ were freshly prepared before each measurement, without purging with N_2 [55]. In a typical experiment, 30 μL of 4-NP (7.5×10^{-3} M) solution were added to the reaction medium (2.8 mL of water) with 200 μL of sodium borohydride solution (0.169 M); the ratio of sodium borohydride to 4-NP concentration in the medium was equal to 150. Under these conditions, all 4-NP was transformed into 4-nitrophenolate (4-NP⁻) which was detected at λ = 400 nm. Then, 0.02 or 0.2 μmol of Re/C or Re/G (the molar amount refers to Re) were added to the solution. Immediately after the addition of the catalyst, time-dependent absorption spectra were recorded at 2 min intervals for two temperatures (35 and 50 °C). The reaction was stopped when the absorbance of 4-NP⁻ did not change with time.

3.3. Microwave-Assisted Oxidation of 1-Phenylethanol

In general, the reaction mixtures were prepared as follows: 2–20 μmol of rhenium catalyst (molar amount refers to rhenium for both the homogeneous and the heterogeneous catalysts) were added to 605 μL (5 mmol) of 1-phenylethanol (substrate) and 1380 μL (10 mmol) of *tert*-butyl hydroperoxide (TBHP, 70% aqueous solution, oxidant). All reactions were run in an added solvent-free system. The focused MW irradiation of the reactional mixture was performed with stirring for 5–60 min at the desired temperature (from 35 to 80 °C). After the reaction, the mixture was cooled to room temperature.

The Re NP-supported catalysts were easily separated from the liquid by centrifugation and filtration, to prepare the samples for GC analysis. The remaining steps are identical for both types of catalysis (supported and homogeneous). Acetonitrile (1 mL) and the internal standard (nitromethane, 50 μL) were added. The obtained mixture was stirred for 5 min and then a sample (1 μL) was taken from the organic phase and analysed by GC. Reactions without catalyst and without oxidant were performed for comparison. Recyclability of the carbon-based catalysts was investigated through their recovery and reuse in consecutive catalytic cycles. A new cycle was initiated after the previous one by addition of new portions of substrate and oxidant. Catalyst recovery was achieved by centrifugation followed by filtration (as above). The products were analysed as above after completion of each run. Rhenium leaching from the carbon support was evaluated throughout the determination of the rhenium content of the recovered solid by ICP-AES before and after reactions.

4. Conclusions

Herein the catalytic activity of synthesized Re NPs immobilized at carbon-based supports (Norit and graphene) was assessed for (i) the formation of 4-aminophenol by reduction 4-nitrophenol, and (ii) the production of acetophenone by oxidative conversion of 1-phenylethanol. For both supported Re catalysts, a small size of Re NPs was achieved, using a simple and fast (5 min) MW-assisted method.

The reduction of 4-nitrophenol to 4-aminophenol was achieved in 30 min, with conversions higher than 80%, and the Re/G catalyst was recycled and reused up to six times with no evident loss of activity. For the 1-phenylethanol oxidation, TONs up to 1.3×10^5 were achieved for Re/G, but its recycling was not possible, due to the occurrence of severe leaching from the carbon support in the oxidative medium. The higher activity of the Re/G catalyst, in both reactions, was attributed to the higher dispersion and smaller particle size of Re NPs when graphene was used as support.

The study shows that Re NPs can act as catalysts for both reduction and oxidation reactions, an unusual type of dual catalytic behaviour.

Moreover, to our knowledge, this is the first time that this type of comparative study between the catalytic activity of Re NPs in different carbon supports, for the same model reactions, is reported**.** Further oxidation reactions and substrates are planned to be tested.

Conflicts of Interest: The authors declare no conflict of interest.

Abbreviations

4-AP—4-aminophenol; 4-NP—4-nitrophenol; C—activated carbon; EDS—energy dispersive spectroscopy; G—graphene; GC—gas chromatography; ICP-AES—inductively coupled plasma atomic emission spectroscopy; MW—microwave; NPs—nanoparticles; OMC—ordered mesoporous carbon; SEM—scanning electron microscopy; TBHP—*tert*-butyl hydroperoxide; TEM—transmission electron microscopy; TOF—turnover frequency; TON—turnover number; XRD—X-ray diffraction.

References

1.　De la Hoz, A.; Diaz-Ortiz, A.; Moreno, A. Microwaves in organic synthesis. Thermal and non-thermal microwave effects. *Chem. Soc. Rev.* **2005**, *34*, 164–178. https://doi.org/10.1039/B411438H.

2.　Kitchen, H.J.; Vallance, S.R.; Kennedy, J.L.; Tapia-Ruiz, N.; Carassiti, L.; Harrison, A.; Whittaker, A.G.; Drysdale, T.D.; Kingman, S.W.; Gregory, D.H. Modern microwave methods in solid-state inorganic materials chemistry: From fundamentals to manufacturing. *Chem. Rev.* **2014**, *114*, 1170–1206. https://doi.org/10.1021/cr4002353.

3.　Gawande, M.B.; Shelke, S.N.; Zboril, R.; Varma, R.S. Microwave-Assisted Chemistry: Synthetic Applications for Rapid Assembly of Nanomaterials and Organics. *Acc. Chem. Res.* **2014**, *47*, 1338–1348. https://doi.org/10.1021/ar400309b.

4.　Chrétien, S.; Buratto, S.K.; Metiu, H. Catalysis by very small Au clusters. *Curr. Opin. Solid State Mater. Sci.* **2007**, *11*, 62–75. https://doi.org/10.1016/j.cossms.2008.07.003.

5.　Yang, X.F.; Wang, A.; Qiao, B.; Li, J.; Liu, J.; Zhang, T. Single-Atom Catalysts: A New Frontier in Heterogeneous Catalysis. *Acc. Chem. Res.* **2013**, *46*, 1740–1748. https://doi.org/10.1021/ar300361m.

6.　Yurkov, G.Y.; Kozinkin, A.V.; Koksharov, Y.A.; Fionov, A.S.; Taratanov, N.A.; Vlasenko, V.G.; Pirog, I.V.; Shishilov, O.N.; Popkov, O.V. Synthesis and properties of rhenium–polyethylene nanocomposite. *Compos. Part B* **2012**, *43*, 3192–3197. https://doi.org/10.1016/j.compositesb.2012.04.019.

7.　Anantharaj, S.; Sakthikumar, K.; Elangovan, A.; Ravi, G.; Karthik, T.; Kundu, S. Ultra-small rhenium nanoparticles immobilized on DNA scaffolds: An excellent material for surface enhanced Raman scattering and catalysis studies. *J. Colloid Interface Sci.* **2016**, *483*, 360–373. https://doi.org/10.1016/j.jcis.2016.08.046.

8.　Dobrzanska-Danikiewicz, A.D.; Wolany, W.; Benke, G.; Rdzawsk, Z. The new MWCNTs–rhenium nanocomposite. *Phys. Status Solidi B* **2014**, *251*, 2485–2490. https://doi.org/10.1002/pssb.201451360.

9.　Aboul-Gheit, A.K.; Abdel-Hamid, S.M.; Aboul-Fotouh, S.M.; Aboul-Gheit, N.A.K. Cyclohexene hydroconversion using monometallic and bimetallic catalysts supported on γ-Alumina. *J. Chin. Chem. Soc.* **2006**, *53*, 793–802. https://doi.org/10.1002/jccs.200600105.

10.　Ni, X.; Zhang, B.; Li, C.; Pang, M.; Su, D.; Williams, C.T.; Liang, C. Hydrogenation of succinic acid over supported rhenium catalysts prepared by the microwave-assisted thermolytic method. *Catal. Commun.* **2012**, *24*, 64–69. https://doi.org/10.1016/j.catcom.2012.03.035.

11.　Di, X.; Shao, Z.; Li, C.; Li, W.; Liang, C. Hydrogenation of succinic acid over supported rhenium catalysts prepared by the microwave-assisted thermolytic method. *Catal. Sci. Technol.* **2015**, *5*, 2441–2448. https://doi.org/10.1039/C5CY00004A.

12.　Bhuyan, M.S.A.; Uddin, M.N.; Islam, M.M. Synthesis of graphene. *Int. Nano Lett.* **2016**, *6*, 65–83. https://doi.org/10.1007/s40089-015-0176-1.

13.　Venkateshaiah, A.; Silvestri, D.; Ramakrishnan, R.K.; Wacławek, S.; Padil, V.V.T.; Černík, M.; Varma, R.S. Gum Kondagoagu/Reduced Graphene Oxide Framed Platinum Nanoparticles and Their Catalytic Role. *Molecules* **2019**, *24*, 3643. https://doi.org/10.3390/molecules24203643.

14.　Rónavári, A.; Igaz, N.; Adamecz, D.I.; Szerencsés, B.; Molnar, C.; Kónya, Z.; Pfeiffer, I.; Kiricsi, M. Green Silver and Gold Nanoparticles: Biological Synthesis Approaches and Potentials for Biomedical Applications. *Molecules* **2021**, *26*, 844. https://doi.org/10.3390/molecules26040844.

15.　Zhang, S.; Xu, Y.; Zhao, D.; Chen, W.; Li, H.; Hou, C. Preparation of Magnetic $CuFe_2O_4$@Ag@ZIF-8 Nanocomposites with Highly Catalytic Activity Based on Cellulose Nanocrystals. *Molecules* **2020**, *25*, 124. https://doi.org/10.3390/molecules25010124.

16.　Shultz, L.R.; McCullough, B.; Newsome, W.J.; Ali, H.; Shaw, T.E.; Davis, K.O.; Uribe-Romo, F.J.; Baudelet, M.; Jurca, T. A Combined Mechanochemical and Calcination Route to Mixed Cobalt Oxides for the Selective Catalytic Reduction of Nitrophenols. *Molecules* **2020**, *25*, 89. https://doi.org/10.3390/molecules25010089.

17.　Hervés, P.; Pérez-Lorenzo, M.; Liz-Marzán, L.M.; Dzubiella, J.; Lu, Y.; Ballauff, M. Catalysis by metallic nanoparticles in aqueous solution: Model reactions. *Chem. Soc. Rev.* **2012**, *41*, 5577–5587. https://doi.org/10.1039/C2CS35029G.

18.　Veerakumar, P.; Dhenadhayalan, N.; Lin, K.C.; Liu. S.B. Highly stable ruthenium nanoparticles on 3D mesoporous carbon: An excellent opportunity for reduction reactions. *J. Mater. Chem. A* **2015**, *3*, 23448–23457. https://doi.org/10.1039/C5TA06875D.

19. He, L.; Wang, L.C.; Sun, H.; Ni, J.; Cao, Y.; He, H.Y.; Fan, K.N. Efficient and selective room-temperature gold-catalyzed reduction of nitro compounds with CO and H2O as the hydrogen source. *Angew. Chem. Int. Ed*. **2009**, *48*, 9538–9541. https://doi.org/10.1002/anie.200904647.

20. Patil, N.M.; Sasaki, T.; Bhanage, B.M. Immobilized iron metal-containing ionic liquid-catalyzed chemoselective transfer hydrogenation of nitroarenes into anilines. *ACS Sustain. Chem. Eng*. **2016**, *4*, 429–436. https://doi.org/10.1021/acssuschemeng.5b01453.

21. Ksu, H.; Ho, S.F.; Metin, C.; Korkmaz, K.; Garcia, A.M.; ltekin, M.S.; Sun, S. Tandem dehydrogenation of ammonia borane and hydrogenation of nitro/nitrile compounds catalyzed by graphene supported NiPd alloy nanoparticles. *ACS Catal*. **2014**, *4*, 1777–1782. https://doi.org/10.1021/cs500167k.

22. Sakai, N.; Fujii, K.; Nabeshima, S.; Ikeda, M.S.; Konakahara. T. Highly selective conversion of nitrobenzenes using a simple reducing system combined with a trivalent indium salt and a hydrosilane. *Chem. Commun*. **2010**, *46*, 3173–3175. https://doi.org/10.1039/C000383B.

23. Mahmoud, M.A.; Garlyyev, B.; El-Sayed, M.A. Determining the mechanism of solution metallic nanocatalysis with solid and hollow nanoparticles: Homogeneous or heterogeneous. *J. Phys. Chem. C* **2013**, *117*, 21886–21893. https://doi.org/10.1021/jp4079234.

24. Antonels, N.C.; Meijboom, R. Preparation of Well-Defined Dendrimer Encapsulated Ruthenium Nanoparticles and Their Evaluation in the Reduction of 4-Nitrophenol According to the Langmuir–Hinshelwood Approach. *Langmuir* **2013**, *29*, 13433–13442. https://doi.org/10.1021/la402885k.

25. Kohantorabi, M.; Gholami, M.R. AgPt nanoparticles supported on magnetic graphene oxide nanosheets for catalytic reduction of 4-nitrophenol: Studies of kinetics and mechanism. *App. Org. Chem*. **2017**, *31*, e3806. https://doi.org/10.1039/C0JM00456A.

26. Gu, S.; Wunder, S.; Lu, Y.; Ballauff, M.; Fenger, R.; Rademann, K.; Jaquet, B.; Zaccone, A. Kinetic analysis of the catalytic reduction of 4-nitrophenol by metallic nanoparticles. *J. Phys. Chem. C* **2014**, *118*, 18618–18625. https://doi.org/10.1021/jp5060606.

27. LiBretto, N.J.; Xu, Y.C.; Quigley, A. Olefin oligomerization by main group Ga^{3+} and Zn^{2+} single site catalysts on SiO2. *Nat. Commun.* **2021**, *12*, 2322. https://doi.org/10.1038/s41467-021-22512-6.

28. Martins, L.M.D.R.S.; Alegria, E.C.B.A.; Smolenski, P.; Kuznetsov, M.L.; Pombeiro, A.J.L. Oxorhenium Complexes Bearing the Water-Soluble Tris(pyrazol-1-yl)methanesulfonate, 1,3,5-Triaza-7-phosphaadamantane, or Related Ligands, as Catalysts for Baeyer–Villiger Oxidation of Ketones. *Inorg. Chem*. **2013**, *52*, 4534. https://doi.org/10.1021/ic400024r.

29. Alegria, E.C.B.; Martins, L.M.D.R.S.; Kirillova, M.V.; Pombeiro. A.J.L. Baeyer-Villiger oxidation of ketones catalyzed by rhenium complexes bearing N- or O-ligands. *Appl. Catal. A Gen*. **2012**, *443–444*, 27–32. https://doi.org/10.1016/j.apcata.2012.07.007.

30. Faísca Phillips, A.M.; Pombeiro, A.J.L.; Kopylovich, M.N. Recent advances in cascade reactions initiated by alcohol oxidation. *ChemCatChem* **2017**, *9*, 217–246. https://doi.org/10.1002/cctc.201601176.

31. Shul'pin, G.B. C–H functionalization: Thoroughly tuning ligands at a metal ion, a chemist can greatly enhance catalyst's activity and selectivity. *Dalton Trans.* **2013**, *42*, 12794–12818. https://doi.org/10.1039/C3DT51004B.

32. Martins, L.M.D.R.S.; Pombeiro, A.J.L. Tris(pyrazol-1yl) methane metal complexes for catalytic mild oxidative functionalizations of alkanes, alkenes and ketones. *Coord. Chem. Rev.* **2014**, *265*, 74. https://doi.org/10.1016/j.ccr.2014.01.013.

33. Martins, L.M.D.R.S. C-scorpionate complexes: Ever young catalytic tools. *Coord. Chem. Rev.* **2019**, *396*, 89. https://doi.org/10.1016/j.ccr.2019.06.009.

34. Alegria, E.C.B.; Kirillova, M.V.; Martins, L.M.D.R.S.; Pombeiro, A.J.L. Pyrazole and Tris(pyrazolyl)methane Rhenium Complexes as Catalysts for Ethane and Cyclohexane Oxidations. *Appl. Catal. A Gen*. **2007**, *357*, 43. https://doi.org/10.1016/apcata.2006.09.038.

35. Kuznetsov, M.L.; Pombeiro, A.J.L. Radical Formation in the [MeReO3]-Catalyzed Aqueous Peroxidative Oxidation of Alkanes: A Theoretical Mechanistic Study. *Inorg. Chem.* **2009**, *48*, 307–318. https://doi.org/10.1021/ic801753t.

36. Kirillov, A.M.; Haukka, M.; Silva, M.F.C.G.; Pombeiro, A.J.L. Preparation and Crystal Structures of Benzoylhydrazido- and-diazenidorhenium Complexes with N,O-Ligands and Their Catalytic Activity Towards Peroxidative Oxidation of Cycloalkanes *Eur. J. Inorg. Chem.* **2005**, *11*, 2071. https://doi.org/10.1002/ejic.200400991.

37. Kirillov, A.M.; Haukka, M.; Kirillova, M.V.; Pombeiro, A.J.L. Single-Pot Ethane Carboxylation Catalyzed by New Oxorhenium(V) Complexes with N,O-Ligands. *Adv. Synth. Catal.* **2005**, *347*, 1435–1446. http://dx.doi.org/10.1002/adsc.200505092.

38. Talsi, E.P.; Bryalov, K.P. Chemo- and stereoselective CH oxidations and epoxidations/cis-dihydroxylations with H2O2, catalyzed by non-heme iron and manganese complexes. *Coord. Chem. Rev.* **2012**, *256*, 1418–1434. https://doi.org/10.1016/j.ccr.2012.04.005.

39. Veerakumar, P.; Thanasekaran, P.; Lin, K.-C.; Liu, S.-B. Well-dispersed rhenium nanoparticles on three-dimensional carbon nanostructures: Efficient catalysts for the reduction of aromatic nitro compounds. *J. Colloid Interf. Sci*. **2017**, *506*, 271–282. https://doi.org/10.1016/j.jcis.2017.07.065.

40. Lee, G.H.; Huh, S.H.; Kim, S.H.; Choi, B.J.; Kim, B.S.; Park, J.H. Structure and size distribution of Os, Re, and Ru nanoparticles produced by thermal decomposition of Os3(CO)12, [Re2(CO)10], and Ru3(CO)12. *J. Korean Phys. Soc.* **2003**, *42*, 835–837.

41. Iben Ayad, A.; Luart, D.; Ould Dris, A.; Guénin, E. Kinetic Analysis of 4-Nitrophenol Reduction by "Water-Soluble" Palladium Nanoparticles. *Nanomaterials* **2020**, *10*, 1169. https://doi.org/10.3390/nano10061169.

42. Soliman, M.M.A.; Kopylovich, M.N.; Alegria, E.C.B.A.; Ribeiro, A.P.C.; Ferraria, A.M.; Botelho do Rego, A.M.; Correia, L.; Saraiva, M.S.; Pombeiro, A.J.L. Ultrasound and radiation-induced catalytic oxidation of 1-phenylethanol to acetophenone with iron-containing particulate catalysts. *Molecules* **2020**, *25*, 740. https://doi.org/10.3390/molecules25030740.

43. Pakrieva, E.; Ribeiro, A.P.C.; Kolobova, E.; Martins, L.M.D.R.S.; Carabineiro, S.A.C.; German, D.; Pichugina, D.; Jiang, C.; Pombeiro, A.J.L.; Bogdanchikova, N.; et al. Supported Gold Nanoparticles as Catalysts in Peroxidative and Aerobic Oxidation of 1-Phenylethanol under Mild Conditions. *Nanomaterials* **2020**, *10*, 151–157. https://doi.org/10.3390/nano10010151.

44. Carabineiro, S.A.C.; Ribeiro, A.P.C.; Buijnsters, J.G.; Avalos-Borja, M.; Pombeiro, A.J.L.; Figueiredo, J.L.; Martins, L.M.D.R.S. Solvent-free oxidation of 1-phenylethanol catalysed by gold nanoparticles supported on carbon powder materials. *Catal. Today* **2020**, *357*, 22–31. https://doi.org/10.1016/j.cattod.2019.06.041.

45. Sousa, S.C.A.; Bernardo, J.R.; Florindo, P.R.; Fernandes, A.C. Efficient and selective oxidation of alcohols catalyzed by oxo-rhenium complexes. *Catal. Commun.* **2013**, *40*, 134–138. https://doi.org/10.1016/j.catcom.2013.06.012.

46. Dimitri, R.; Teresa, G.; Corrado, C.; Erica, F. Iron-Catalyzed Oxidation of 1-Phenylethanol and Glycerol With Hydrogen Peroxide in Water Medium: Effect of the Nitrogen Ligand on Catalytic Activity and Selectivity. *Front. Chem.* **2020**, *8*, 810–823. https://doi.org/10.3389/fchem.2020.00810.

47. Carbon Based Materials Surface Data. Available online: https://www.sigmaaldrich.com (accessed on 23 February 2022).

48. Pombeiro, A.J.L.; Martins, L.M.D.R.S.; Ribeiro, A.P.C.; Carabineiro, S.A.C.; Figueiredo, J.L. Production Process of Ketones from Secondary Alcohols. WO 2017/116253, PCT/PT2016/000019, PT109062, 29 December 2015.

49. Martins, L.M.D.R.S.; Ribeiro, A.P.C.; Carabineiro, S.A.C.; Figueiredo, J.L.; Pombeiro , A.J.L. Highly efficient and reusable CNT supported iron(II) catalyst for microwave assisted alcohol oxidation. *Dalton Trans.* **2016**, *45*, 6816–6819. https://doi.org/10.1039/C6DT00514D.

50. Ribeiro, A.P.C.; Martins, L.M.D.R.S.; Carabineiro, S.A.C.; Buijnsters, J.G.; Figueiredo, J.L.; Pombeiro, A.J.L. Heterogenised C-scorpionate iron(II) complex on nanostructured carbon materials as catalysts for microwave-assisted oxidation reactions. *ChemCatChem* **2018**, *10*, 1821–1828. https://doi.org/10.1002/cctc.201702031.

51. Payra, S.; Challagulla, S.; Chakraborty, C.; Roy, S. A hydrogen evolution reaction induced unprecedentedly rapid electrocatalytic reduction of 4-nitrophenol over ZIF-67 compare to ZIF-8. *J. Electroanal. Chem.* **2019**, *853*, 113545. https://doi.org/10.1016/j.jelechem.2019.113545.

52. WWAP (UNESCO World Water Assessment Programme). *The United Nations World Water Development Report 2019: 34 Leaving No One Behind*; UNESCO: Paris, France, 2019.

53. Zheng, Y.; Liu, D.; Liu, S.; Xu, S.; Yuan, Y.; Xiong, L. Kinetics and mechanisms of p-nitrophenol biodegradation by *Pseudomonas aeruginosa* HS-D38. *J. Environ. Sci.* **2009**, *21*, 1194–1199. https://doi.org/10.1016/S1001-0742(08)62403-1.

54. United States Environmental Protection Agency. *Health Effects Assessment for Nitrophenols*; United States Environmental Protection Agency: Washington, DC, USA, 1987.

55. Wunder, F.; Lu, Y.; Albrecht, M. Catalytic activity of facetted gold nanoparticles studied by a model reaction: Evidence for substrate-induced surface restructuring. *ACS Catal.* **2011**, *1*, 908–916. https://doi.org/10.1021/cs200208a.

56. Iskandar, F.; Hikmah, U.; Stavilab, E.; Aimona, A.H. Microwave-assisted reduction method under nitrogen at-mosphere for synthesis and electrical conductivity improvement of reduced graphene oxide (rGO). *RSC Adv.* **2017**, *7*, 52391.